AGU PUBLICATIONS

Geophysical Research Letters

RESEARCH LETTER
10.1002/2013GL059079

Key Points:
- CO_2 forcing increases meridional gradient in net radiation
- Forcing, rather than feedback, accounts for enhanced poleward energy transport
- Aerosol forcing accounts for an inter-hemispheric transport anomaly

Correspondence to:
Y. Huang,
Yi.Huang@mcgill.ca

Citation:
Huang, Y., and M. Zhang (2014), The implication of radiative forcing and feedback for meridional energy transport, *Geophys. Res. Lett.*, *41*, 1665–1672, doi:10.1002/2013GL059079.

Received 18 DEC 2013
Accepted 7 FEB 2014
Accepted article online 11 FEB 2014
Published online 4 MAR 2014

The implication of radiative forcing and feedback for meridional energy transport

Yi Huang[1] and Minghong Zhang[1]

[1]Department of Atmospheric and Oceanic Sciences, McGill University, Montreal, Quebec, Canada

Abstract The distributions of radiative forcing and feedback in the Coupled Model Intercomparison Project phase 5 abrupt4xCO2 and Historical experiments are diagnosed, with a focus on their effects on the zonal mean structure of the top-of-the-atmosphere radiation anomalies and implications for the meridional energy transport. It is found that because the greenhouse gas longwave forcing peaks in the low latitudes, it reinforces the equator-to-pole net radiation gradient and accounts for the increase in the poleward energy transport in both hemispheres under global warming. The shortwave forcing by aerosol, ozone, etc. peaks in the Northern Hemisphere and instead implies an interhemispheric energy transport. Although the water vapor feedback also reinforces the equator-to-pole gradient of the net radiation, the temperature and albedo feedback act against it. The feedback tend to offset the zonal mean radiation anomaly caused by the forcing, although the overall feedback effect on the energy transport is rather uncertain, mainly due to the uncertainty in the cloud feedback.

1. Introduction

The atmospheric and oceanic circulations transport energy poleward in order to balance the top-of-the-atmosphere (TOA) net radiation surplus in the low latitudes and the deficit in the high latitudes. An increased poleward energy transport appears a robust feature of the general circulation model (GCM) simulations in global warming experiments [*Held and Soden*, 2006; *Hwang and Frierson*, 2010]. As the meridional energy transport (MET) connects climate system across different latitudes, a change in the transport may have profound impacts on regional weather and climate, such as the amplification of surface warming in the polar region [*Hu et al*., 2004; *Lu and Cai*, 2010] and shifts in the Intertropical Convergence Zone [*Kang et al*., 2008; *Hwang et al*., 2013].

From an energy balance point of view, an increasing trend in the poleward energy transport implies that the radiative surplus and deficit in the low and high latitudes, respectively, have become larger than the climatological values. *Wu et al*. [2010] show that the enhanced poleward energy transport in a warmer climate is associated with an anomalous energy gain in the tropical atmosphere relative to the high latitudes. *Zelinka and Hartmann* [2012] attribute the energy gain in the low latitudes to the water vapor and cloud feedback, which are strongly positive (inducing less outgoing radiation at higher surface temperature) at low latitudes and decrease dramatically toward higher latitudes in their analysis of the Coupled Model Intercomparison Project phase 3 (CMIP3) models.

Regional differences in feedback have been noticed between different models and between different scenario experiments [*Huang*, 2013; *Vial et al*., 2013; *Zhang and Huang*, 2013]. Hence, it calls into question how robust the feedback effect on the latitudinal (zonal mean) radiation anomaly distribution and thus the energy transport is. Moreover, it has been recognized that the radiative forcing is model dependent and also has a strongly nonuniform geographical distribution [*Collins et al*., 2008; *Dufresne and Bony*, 2008; *Forster et al*., 2013; *Huang*, 2013; *Zhang and Huang*, 2013]. It is important to elucidate how the forcing modifies the radiation energy budget balance in different latitudes and whether it demands a change in MET as well.

In this study, we analyze the latitudinal structures of forcing and feedback in the CMIP5 GCMs using the diagnostic method developed by *Huang* [2013] and *Zhang and Huang* [2013] and assess their implications for the MET.

2. Method

2.1. Experiments and Models

Our analysis is based on two CMIP5 experiments: abrupt4xCO2 and Historical experiments [*Taylor et al*., 2013]. In the abrupt4xCO2 experiment, the atmospheric CO_2 concentration is abruptly quadrupled from the

preindustrial level and then maintained at the high level in a 150 year integration of fully coupled atmosphere-ocean GCMs. The Historical experiment is integrated from the preindustrial to the present day (1860 to 2005), forced by prescribed historical values of various forcing species. The two experiments provide all-at-once forced, equilibrium-approaching and more gradually forced, nonequilibrium (transient) scenarios, respectively, for examining the forcing and feedback effects under investigation here. The difference between the last 10 years of the 150 years abrupt4xCO2 integration and the 30 years preindustrial control climatology is calculated as the climate response to the quadrupling of CO_2. The climate change in the Historical experiment is calculated as the long-term linear trend over the 1860–2005 period. The models analyzed for the abrupt4xCO2 experiment include 11 models that provide sufficient data for the radiative feedback analysis: GFDL-CM3, IPSL-CM5A-LR, HaadGEM2-ES, CCSM4, CanESM2, MRI-CGCM3, MPOI-ESM-MR, CISRO-Mk-6-0, INMCM4, MIROC5, and NorESM1-M (see Table 9.A.1 of the fifth Intergovernmental Panel on Climate Change assessment report for details of these models); for the Historical experiment, same as abrupt4xCO2 except that CCSM4 is omitted and that the GFD-ESM2M model is added.

2.2. Forcing and Feedback Analysis

Our forcing analysis is based on the "stratosphere-adjusted" forcing that consists the instantaneous forcing and the stratospheric adjustment, both measured with the TOA radiative flux. We use the method first proposed by *Huang* [2013] to determine the radiative forcing in each model. This method is based on the decomposition of the overall change in the TOA radiation flux ΔR.

First, the clear-sky radiative forcing including the stratosphere adjustment is obtained based on the decomposition of the overall change in the clear-sky radiation:

$$F^{clr} = \Delta R^{clr} - \left(\Delta {R_{Ts}}^{clr} + \Delta {R_T}^{clr} + \Delta {R_W}^{clr}\right) \tag{1}$$

ΔR^{clr} is the model-simulated clear-sky overall radiation change; the contributions by surface temperature (T_S), tropospheric temperature (T) , and water vapor (W) are quantified through the kernel method [*Soden et al*., 2008; *Shell et al*., 2008].

Then, we apply a cloud forcing (the difference between R and R^{clr}) scaling to obtain the all-sky forcing F:

$$\frac{F^{clr} - F}{\left(F^{clr}\right)_{ref}} = \frac{0.16}{1.16} \cdot \frac{CF}{(CF)_{ref}} \tag{2}$$

The reference clear-sky forcing $(F^{clr})_{ref}$ and cloud forcing $(CF)_{ref}$ are taken to be the multimodel ensemble mean of the global mean of these quantities. The method provides radiative forcing in each grid box for each model (see *Zhang and Huang* [2013] for the details and validation of the method). In the following we denote the longwave stratosphere-adjusted radiative forcing LF and the shortwave radiative forcing SF. As the CO_2 forcing is mostly exerted on the longwave radiation, we discuss only LF for the abrupt4xCO2 experiment.

We use the radiative kernels of *Soden et al*. [2008] and *Shell et al*. [2008] to obtain the noncloud contributions (feedback) to the all-sky total radiation change. The cloud feedback is then measured as the residual in the all-sky radiation budget [*Zhang and Huang*, 2013]:

$$\Delta R_C = \Delta R – (F + \Delta R_{T_{\mathrm{tr}}} + \Delta R_{W_{\mathrm{tr}}} + \Delta R_A) \tag{3}$$

which is equivalent to applying the cloud forcing adjustment method [*Soden et al*., 2008; *Shell et al*., 2008] with explicitly assessed radiative forcing.

2.3. Implied MET

Then, we take the geographic distribution of the radiation anomaly caused by each forcing or feedback component and calculate its implied MET anomaly (that would be demanded by the need of balancing the net radiation at every latitude) through a northward integration [*Hartmann*, 1994, equation (2.21)]:

$$F(\phi) = \int_{-\frac{\pi}{2}}^{\phi} \int_0^{2\pi} R_X'(\lambda, \phi) \alpha^2 \cos\phi \, \mathrm{d}\lambda \, \mathrm{d}\phi \tag{4}$$

Here $F(\phi)$ is the anomalous northward energy flux across a latitude circle, ϕ is latitude, λ is longitude, α is the radius of the earth, and $R_X'(\lambda, \phi)$ is the TOA radiative flux anomaly due to each forcing or feedback component, minus its global mean value and normalized by the global mean surface temperature anomaly in each model. Note that the normalization is also done to the forcing in order to compare the effect of forcing

and feedback across different models. The net MET can be further decomposed between the atmosphere and ocean by taking into account the surface energy flux anomalies. The implied atmospheric poleward transport is given as

$$F_{\mathrm{atm}}(\phi) = \int_{-\frac{\pi}{2}}^{\phi} \int_{0}^{2\pi} \left[R'(\lambda, \phi) + Q'(\lambda, \phi)\right] \alpha^2 \cos\phi \, \mathrm{d}\lambda \mathrm{d}\phi \tag{5}$$

where $F_{\mathrm{atm}}(\phi)$ is the anomalous northward atmospheric energy flux across a latitude circle, and $R'(\lambda,\phi)$ and $Q'(\lambda,\phi)$ are the surface temperature-normalized net TOA and surface flux anomalies, respectively.

3. Results

3.1. The Quadrupling CO_2 Experiment

Figure 1 shows the ensemble mean LF, feedback, and implied northward energy transport diagnosed from the abrupt4xCO2 experiment. Although the CO_2 concentration and perturbation are prescribed to be uniform across the globe in this experiment, it is clear from Figure 1a that the stratosphere-adjusted forcing has a nonuniform latitudinal distribution and a noticeable intermodel spread in the forcing magnitude (see *Zhang and Huang*, 2013, Figure 4 for the geographic distribution of the forcing and the discussions there on the intermodel spread). The forcing generally decreases from low latitudes to high latitudes due to the Planck effect (To the first order, the greenhouse effect is proportional to the surface emission and thus is less at lower temperatures.); the abundant clouds and water vapor in the deep convective regions (e.g., the Intertropical Convergence Zone) result in local minima of the forcing due to their masking effects. Consequently, the zonal mean radiative forcing induced TOA radiation anomaly is the greatest in the tropics and declines from approximately 1.8 W m^{-2} K^{-1} in the subtropics to 0.8 W m^{-2} K^{-1} at the poles (Figure 1a). This gradient in forcing reinforces the preexisting latitudinal gradient in the TOA net radiation, implying an interhemispherically symmetric, enhanced poleward energy flux that diverges energy from the tropics to poles (Figure 1b).

The sum of climate feedback in the abrupt4xCO2 experiment is negative at all latitudes (see Figure 1a, blue line), indicating that the net feedback is to damp the warming effect of the radiative forcing. The temperature, water vapor, and cloud feedback diagnosed from this experiment (Figures 1c and 1e) exhibit very similar zonal mean structures to those diagnosed from the CMIP3 A2 experiment by *Zelinka and Hartmann* [2012]. The equator-to-pole gradient in water vapor feedback is largely offset by the temperature feedback at most latitudes. The surface albedo feedback is positive and confined to high latitudes. The ensemble mean net cloud feedback is positive between 60°N and 50°S and negative in high latitudes, largely dominated by the SW component except in the deep tropics. However, the overall feedback effect (Figure 1a, blue line) and its implied MET (Figure 1b) are noticeably different from the results of *Zelinka and Hartmann* [2012]. The discrepancy comes from the relatively weaker equator-to-pole gradient in both water vapor and cloud feedback and considerably stronger opposite gradient induced by the surface albedo feedback in the results here. It is possible that the difference results from the different forcings between the equilibrium-approaching abrupt4xCO2 and the transient A2 experiments. For example, the stronger surface albedo feedback in the abrupt4xCO2 experiment is likely due to continued amplification of warming in the polar regions in both hemispheres over the decades following the perturbation, which is not fully attained in the A2 experiment [e.g., *Manabe et al*., 1991; *Armour et al*., 2013].

From Figure 1a, it is clear that the forcing and feedback both considerably modify the zonal mean structure of net radiation distribution and thus have a strong implication for the MET (Figure 1b). While the forcing effect is persistent and similar in the models and requires more poleward energy transport in both hemispheres, the net feedback effect has a larger intermodel spread but generally acts to reduce the change in energy transport that is implied by the forcing effect. The zonal mean structure of the overall radiation anomaly, after considering both effects, exhibits three peaks, which can be traced to a combination of water vapor and cloud feedback at the equator and the surface albedo feedback near the poles. The energy flux anomalies implied by the net radiation change is to transport the anomalous net radiative energy out of these regions.

3.2. The Historical Experiment

The LF derived from the Historical experiment (Figure 2a) shows a similar distribution pattern to the aburpt4xCO2 experiment and thus also leads to enhanced northward energy transport. The SF (Figure 2b) exhibits a much less uniform distribution with maxima over the continents where the aerosols emission

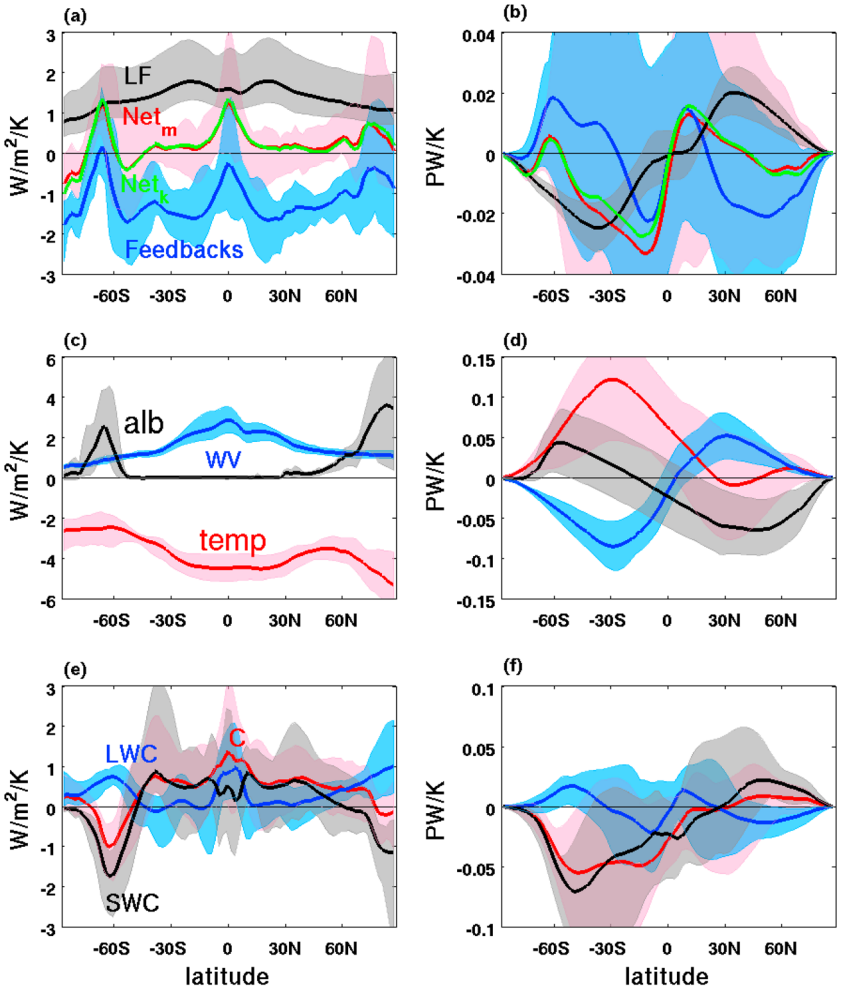

Figure 1. (a) Zonal mean structures of multimodel mean TOA radiation flux anomalies (red: model simulated; green: sum of analyzed forcing and feedback), total radiative forcing (black), and sum of climate feedback (blue) and (b) their implied northward meridional energy flux anomalies derived from abrupt4xCO2 experiment. (c and d) Same as Figures 1a and 1b but for temperature (red), water vapor (blue), and surface albedo (black) feedback. (e and f) Same as Figures 1a and 1b but for the net (red), LW (blue), and SW (black) cloud feedback. The thick line represents the multimodel mean, and the corresponding shading represents the intermodel spread. Note the forcing values are normalized by global mean surface temperature anomaly for comparison with the feedback.

peaks and noticeable signals over the Antarctic, which are likely caused by the ozone loss and thus decrease in the absorption of SW radiation [*Shindell et al.*, 1998; *Staehelin et al.*, 2001]. As a result, the zonal mean structure of the SF shows an interhemispheric asymmetry with the most negative value in the northern midlatitudes, requiring the meridional heat flux to converge there. The surface temperature change-normalized radiative forcing (in the unit of W $m^{-2} K^{-1}$) is noticeably larger in the Historical experiment than in the abrupt4xCO2 experiment because of the transient (nonequilibrium) nature of the experiment (the warming of the surface by the radiative forcing has not been fully attained) and a smaller time-integrated forcing in this experiment.

The climate feedback (Figure 2c) in the Historical experiment show somewhat different structures from the more idealized abrupt4xCO2 experiment. There is a large intermodel spread in zonal mean cloud feedback (Figure 2i), as disclosed by many previous studies. The temperature feedback (Figure 2g) shows an interhemispheric asymmetry due to delayed warming in southern high latitudes in contrast to the amplification of warming in the Arctic [e.g., *Manabe et al.*, 1991].

The feedback offsets the net radiation anomaly caused by the forcing in the Historical experiment, like in the abrupt4xCO2 experiment. However, the offset is less exact, and there is much more interhemispheric

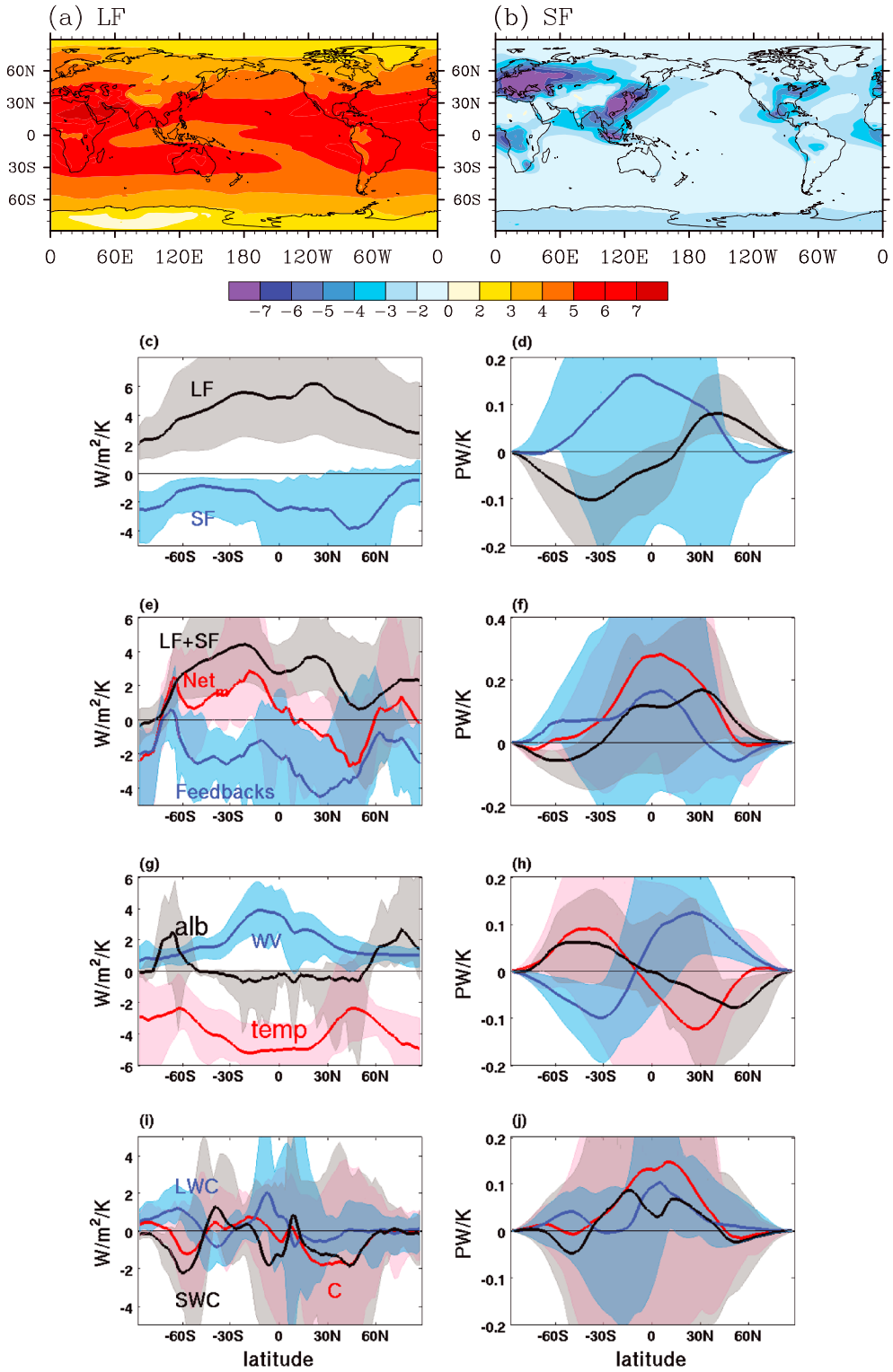

Figure 2. Geographic distribution of the multimodel ensemble mean of (a) longwave and (b) shortwave forcing derived from the Historical experiment. (c) Their zonal mean structures and (d) their implied northward meridional energy flux anomalies. (e) Zonal mean structures of multimodel mean TOA radiation flux anomalies (red), total radiative forcing (black), and sum of climate feedback (blue) and (f) their implied northward meridional energy flux anomalies. (g and h) Same as Figures 2e and 2f but for temperature (red), water vapor (blue), and surface albedo (black) feedback. (i and j) Same as Figures 2e and 2f but for the net (red), LW (blue), and SW (black) cloud feedback. Lines and shadings represent multimodel ensemble mean and spread, respectively.

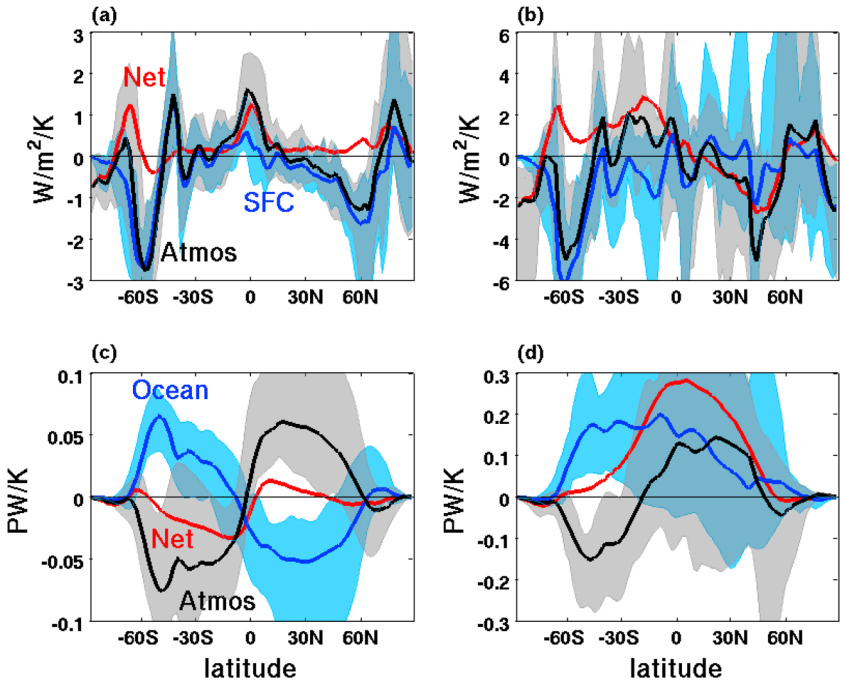

Figure 3. Multiple-model mean anomalies in the TOA net radiation (red), surface flux (blue), and net flux into atmosphere (black) derived from the (a) abrupt4xCO2 and (b) Historical experiments. (c and d) The implied changes in northward energy transport in the two experiments, respectively, partitioned into atmospheric (black) and oceanic (blue) components. Shadings indicate the intermodel spread. Note that positive values represent anomalous fluxes into the atmosphere.

asymmetry in the net radiation anomaly after considering both effects. As a result, a northward energy transport from Southern Hemisphere to Northern Hemisphere is required, to which the primary contributors can be traced to the shortwave forcing and cloud feedback (though with much uncertainty as indicated by intermodel spread).

3.3. Atmospheric Transport

Figure 3 shows the partition of the implied MET between ocean and atmosphere after taking into consideration the surface flux anomalies (see equation (5)). In the abrupt4xCO2 experiment, there is an increase of about 0.33 W m^{-2} K^{-1} in the multimodel global mean total energy flux (including radiative, sensible, and latent energy fluxes) into the Earth's surface. The downward fluxes mainly occur in the subpolar regions, while at most other latitudes the flux is upward, into the atmosphere. Hence, the surface flux anomaly structure acts to preferentially heat the tropical atmosphere relative to the high latitudes, which means more atmospheric poleward transport is required.

In the Historical experiment, the increase in the energy flux into the surface is about 0.84 W m^{-2} K^{-1} on global average and mainly occurs in the southern subpolar region (mainly contributed by the sensible heat flux, not shown). The surface flux anomaly structure demands an atmospheric energy transport from the equator toward the South Pole and an opposite transport in the ocean to balance their individual energy budgets. A noteworthy difference compared to the abrupt4xCO2 experiment is that the surface heat flux is not as negative (positive means into the atmosphere) over the northern midlatitudes, which is related to a net upward shortwave radiation flux anomaly, likely caused by the absorption and reflection of aerosols. Given that the TOA radiation anomaly requires northward energy transport in both hemispheres, it is interesting that the implied atmospheric transport is poleward in both hemispheres, as in the abrupt4xCO2 experiment. This can be explained by the increase in moist static energy gradient in a warmer climate caused by faster increase in latent energy in lower latitudes [*Hwang and Frierson*, 2010]. The peak value of the atmospheric transport is roughly 0.06 (0.15) Petawatt (PW) per degree of global mean temperature increase in the abrupt4xCO2 (Historical) experiment. Considering the global warming simulated by the

models is 5.11 (0.6) K, these flux changes are about 10% (3%) as large as the climatological atmospheric flux in low latitudes [cf. *Trenberth and Caron*, 2001, Figure 7].

4. Conclusion

We diagnose the radiative forcing and feedback distributions in the CMIP5 Abrupt4xCO2 and Historical experiments and investigate the latitudinal structures of the TOA radiation anomalies due to each of these effects and their implications for the MET as the planet warms.

Our study finds that the latitudinal gradient in greenhouse gas longwave forcing reinforces the mean equator-to-pole net radiation gradient and by itself requires the climate system to transport more energy poleward. The shortwave forcing by aerosol, ozone, etc. modifies the implication for the MET and by itself requires an interhemispheric transport.

It is found that the net feedback effect tends to offset the TOA radiation anomaly caused by the forcing. The offset, however, is somewhat delicate so that the resulted latitudinal gradient of net radiation anomaly and thus the implied MET are uncertain. While an increase in poleward transport is required in both hemispheres to transport the anomalous energy from the tropics to the extratropics in the idealized Abrupt4xCO2 experiment, anomalous energy is required to be transported from the Southern Hemisphere to the Northern Hemisphere in the Historical experiment.

Although the water vapor feedback demands an increase in equator-to-pole transport, the temperature and albedo feedback compensate it. There is much uncertainty, reflected by both intermodel and interscenario differences, on the latitudinal structure of the cloud feedback and thus its implication for the MET.

Interestingly, when the implied change in the overall energy transport is partitioned into atmospheric and oceanic components, it is found that although the change in the oceanic transport differs between the scenarios, the atmosphere is always required to perform more poleward energy transport.

Acknowledgments

We thank Tim Merlis, Yutian Wu, Daniel Feldman, and two anonymous reviewers whose comments have helped improve the paper. This work is supported by a Discovery grant from the Natural Sciences and Engineering Research Council of Canada.

The Editor thanks two anonymous reviewers for their assistance in evaluating this paper.

References

Armour, K. C., C. M. Bitz, and G. H. Roe (2013), Time-varying climate sensitivity from regional feedbacks, *J. Clim.*, *26*, 4518–4534, doi:10.1175/JCLI-D-12-00544.1.

Collins, W. D., et al. (2008), Radiative forcing by well-mixed greenhouse gases: Estimates from climate models in the Intergovernmental Panel on Climate Change (IPCC) Fourth Assessment Report (AR4), *Geophys. Res. Lett.*, *111*, D14317, doi:10.1029/2005JD006713.

Dufresne, J.-L., and S. Bony (2008), An assessment of the primary sources of spread of global warming estimates from coupled atmosphere–ocean models, *J. Clim.*, *21*, 5135–5144.

Forster, P. M., T. Andrews, P. Good, J. M. Gregory, L. S. Jackson, and M. Zelinka (2013), Evaluating adjusted forcing and model spread for historical and future scenarios in the CMIP5 generation of climate models, *J. Geophys. Res. Atmos.*, *118*, 1139–1150, doi:10.1002/jgrd.50174.

Hartmann, D. L. (1994), *Global Physical Climatology*, 411 pp., Academic Press, San Diego, Calif.

Held, I. M., and B. J. Soden (2006), Robust responses of the hydrological cycle to global warming, *J. Clim.*, *19*, 5686–5699.

Huang, Y. (2013), On the longwave climate feedbacks, *J. Clim.*, *26*, 7603–7610, doi:10.1175/JCLI-D-13-00025.1.

Hu, A., G. A. Meehl, W. M. Washington, and A. Dai (2004), Response of the Atlantic thermohaline circulation to increased atmospheric CO2 in a coupled model, *J. Clim.*, *17*, 4267–4279, doi:10.1175/JCLI3208.1.

Hwang, Y.-T., and D. M. W. Frierson (2010), Increasing atmospheric poleward energy transport with global warming, *Geophys. Res. Lett.*, *37*, L24807, doi:10.1029/2010GL045440.

Hwang, Y.-T., D. M. W. Frierson, and S. M. Kang (2013), Anthropogenic sulfate aerosol and the southward shift of tropical precipitation in the late 20th century, *Geophys. Res. Lett.*, *40*, 2845–2850, doi:10.1002/grl.50502.

Kang, S. M., I. M. Held, D. M. W. Frierson, and M. Zhao (2008), The response of the ITCZ to extratropical thermal forcing: Idealized slab-ocean experiments with a GCM, *J. Clim.*, *21*(14), 3521–3532.

Lu, J., and M. Cai (2010), Quantifying contributions to polar warming amplification in an idealized coupled general circulation model, *Clim. Dyn.*, *34*(5), 669–687.

Manabe, S., R. J. Stouffer, M. J. Spelman, and K. Bryan (1991), Transient responses of a coupled ocean–atmosphere model to gradual changes of atmospheric CO2. Part I. Annual mean response, *J. Clim.*, *4*, 785–818.

Shell, K. M., J. T. Kiehl, and C. A. Shields (2008), Using the radiative kernel technique to calculate climate feedbacks in NCAR's Community Atmospheric Model, *J. Clim.*, *21*, 2269–2282.

Soden, B. J., I. M. Held, R. Colman, K. M. Shell, J. T. Kiehl, and C. A. Shields (2008), Quantifying climate feedbacks using radiative kernels, *J. Clim.*, *21*, 3504–3520.

Staehelin, J., N. R. P. Harris, C. Appenzeller, and J. Eberhard (2001), Ozone trends: A review, *Rev. Geophys.*, *39*(2), 231–290.

Shindell, D. T., D. Rind, and P. Lonergan (1998), Increased polar stratospheric ozone losses and delayed eventual recovery owing to increasing greenhouse-gas concentrations, *Nature*, *392*(6676), 589–592.

Taylor, P. C., M. Cai, H. Aixue, J. Meehl, W. Washington, and G. J. Zhang (2013), A decomposition of feedback contributions to Polar warming amplification, *J. Clim.*, *26*, 7023–7043.

Trenberth, K. E., and J. M. Caron (2001), Estimates of meridional atmosphere and ocean heat transports, *J. Clim.*, *14*, 3433–3443.

Vial, J., J.-L. Dufresne, and S. Bony (2013), On the interpretation of inter-model spread in CMIP5 climate sensitivity estimates, *Clim. Dyn.*, *41*, 3339–3362, doi:10.1007/s00382-013-1725-9.

Wu, Y., M. Ting, R. Seager, H.-P. Huang, and M. Cane (2010), Changes in storm tracks and energy transports in a warmer climate simulated by the GFDL CM2.1 model, *Clim. Dyn.*, *37*, 53–72, doi:10.1007/s00382-010-0776-4.

Zelinka, M. D., and D. L. Hartmann (2012), Climate feedbacks and their implications for poleward energy flux changes in a warming climate, *J. Clim.*, *25*, 608–624.

Zhang, M., and Y. Huang (2013), Radiative forcing of quadrupling CO_2, *J. Clim.*, doi:10.1175/JCLI-D-13-00535.1.